Numerical study on the response of composite shear walls with steel sheets under cyclic loading

[1]M. Nadir Olabi, [*2]Naci Caglar, [1,3]M. Hasim Kisa, and [4]S. Bahadir Yuksel

[1] *Department of Civil Engineering, Institute of Natural Sciences, Sakarya University, 54050 Sakarya, TURKEY*
[2] *Department of Civil Engineering, Faculty of Engineering, Sakarya University, 54050 Sakarya, TURKEY*
[3] *Department of Civil Engineering, Faculty of Engineering, Karabuk University, 78050 Karabuk, TURKEY*
[4] *Department of Civil Engineering, Engineering and Natural Sciences Faculty, Konya Technical University, Konya, TURKEY*

Abstract

As an alternative to conventional reinforced concrete walls, composite shear walls have been studied recently due to their great advantages in terms of structural performance under seismic loading. Researchers usually use ready-made profiles for composite shear walls, but in this study L-shaped cold-formed steel sheets were selected for numerical analysis under lateral cyclic forces. A macroscale numerical model was developed using a fiber beam-column element with a shear spring model to reproduce the actual behavior of composite shear walls. In addition, the OpenSees-based model was verified against three experimentally tested composite shear walls and showed robust simulation ability. Moreover, in order to fully explain their effect on the performance of composite shear walls, the properties of L-shaped steel sheets were studied parametrically with the help of the numerical model in terms of thickness and yield strength. It was clear that increases in the sheets' yield strength and thickness increased the lateral load-displacement capacity of the walls. It was thought that the two factors were connected in terms of their effects, and the L-shaped steel sheet arrangement in the boundary zone had essential participation in the total response of the composite shear wall under the applied loads.

Keywords: composite RC shear walls, L-shaped cold-formed steel sheets, fiber beam-column element, macroscopic model, OpenSees.

* Corresponding Author: N. Caglar, caglar@sakarya.edu.tr

1. Introduction

Reinforced concrete (RC) shear walls are generally used in high-rise buildings subjected to earthquakes. The high-rise buildings require more lateral load capacities and stiffness than conventional shear walls can offer due to the excessive moment and axial load effects. Shear wall cross-section properties require dense reinforcement and rather thick concrete sections with the effect of internal loads, resulting in limited usable floor space. To tackle these problems, composite shear walls have been used recently for lateral load-resistant elements as the main part of the load-bearing system in high-rise buildings [1]. Researchers proposed the use of different types of composite shear wall elements which had ready-made profiles and steel sections [2-3]. Within this scope, a lot of experimental studies have been conducted to understand the response of composite shear walls subjected to lateral loads [1, 4-9]. Alternatively, Yuksel and Unal [10] proposed L-shaped cold-formed steel sheets (CFSS) instead of ready-made steel profiles to create the composite shear walls. Kisa and Kisa et al. [11-12] performed an experimental study to determine the effects of different configurations of L-shaped CFSS on the total response of the composite shear wall.

On the other hand, numerical analyses on composite shear walls have been also investigated by many researchers. In this context, Wang et al. [13] conducted a numerical analysis on steel plate reinforced concrete composite shear walls using OpenSees software. The authors of this work performed a parametric study depending on axial load ratio, steel plate ratio, concrete strength, and web steel ratio. Elmatzoglou and Avdelas [14] focused on numerical analyses of double-steel plate composite shear walls. In their study, short analyzing time and high accuracy were desired for the calculations. Nguyen and Whittaker [15] modeled steel-plate concrete composite shear walls with a microscopic approach, thus the main design parameters of the shear wall were considered in detail. Zhou et al. [16] examined the lateral load capacity of composite shear walls containing double steel plates and filled concrete with binding bars, and a method was also developed for estimating the load capacities of shear walls. Cho et al. [17] performed a nonlinear static analysis to determine the seismic capacity of steel plate concrete shear walls, and an analytical approach was developed to model the nonlinear behavior of the SC shear wall. The authors reported that more accurate analytical result requires well-defined contact elements between concrete and studs. Ali et al. [18] investigated the modeling of nonlinear behavior of an I-shaped composite steel-concrete shear wall under reversible loads. The researchers suggested the usage of steel plate elements in the section body instead of flanges as a cost-efficient solution. Moreover, the authors mentioned the absence of pinching effect in the force-displacement curve because of the difficulties to model the dense geometry and bond behavior of walls. Zhou et al. [19] carried out a nonlinear numerical analysis to estimate the hysteretic response of composite shear walls. They also developed a quadric-linear skeleton curve model to predict the load-bearing capacity. However, there is a limited investigation about numerical analysis of composite shear walls with L-shaped cold-formed steel sheets.

In this paper, a numerical parametric study was conducted using OpenSees software [20] to understand the response of composite shear walls with L-shaped cold-formed steel sheets better. Moreover, yielding strength and thickness of CFSS were selected as the main variables of the parametric study. It was very important to validate the OpenSees model with experimental results to test the accuracy of the analytical model in predicting the overall behavior of composite shear walls under cyclic lateral loads. The three composite RC walls reported by Yuksel and Unal [10] (CSW1), Kisa, and Kisa et al. [11-12] (CSW2, CSW3) were selected to confirm the numerical model. Although the predicted maximum lateral loads were in good conformity with the experimental test data, numerical models overestimated the initial lateral stiffness at small displacement levels before reaching the peak load. On the contrary, the calculated dissipated energy was in a very good harmony between the numerical and experimental curves. The paper includes determinations of the numerical analysis process, deformation and load-bearing capacity, and effect of the main steel variables on composite shear walls.

2. Experimental study

The experimental program was conducted in the Earthquake Laboratory at Selçuk University, Turkey, and consisted of three 1:3 scaled composite shear walls (CSW) with cold-formed steel sheets installed in walls boundary zones. The details of the cross-section of the test wall specimens are shown in Fig. 1.

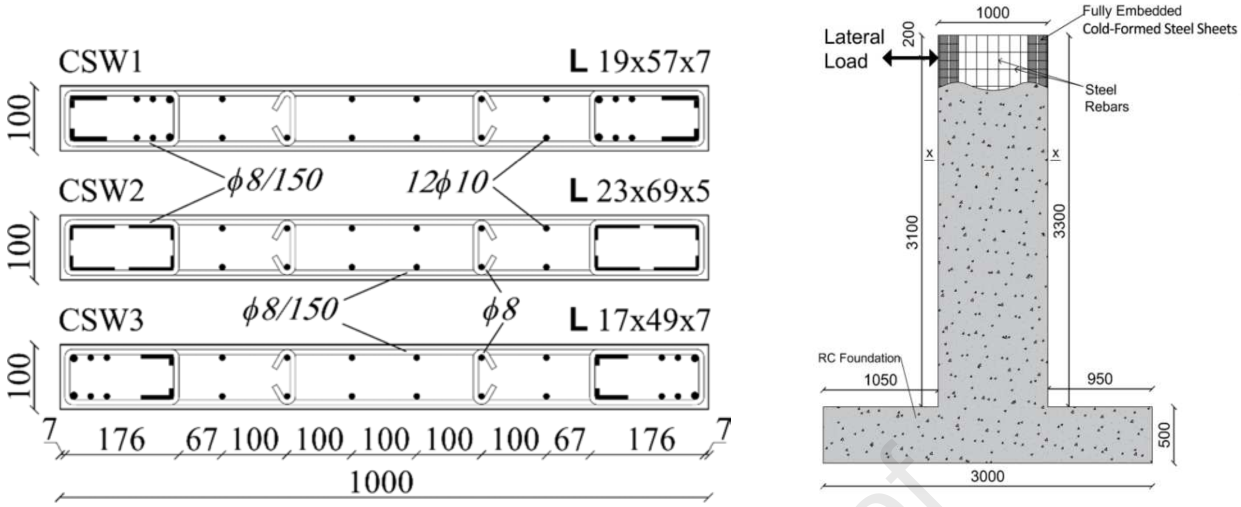

a) Cross sections and reinforcement details

b) Wall and base dimensions

Fig. 1 Details of CSW test specimens

The specimen's thickness and length were selected as 100 mm and 1000 mm, respectively. The height of the walls was 3300 mm and the cyclic lateral load was applied at 3100 mm from the surface of the RC foundation. The shear wall base was fixed to the rigid floor with eight tie rods. In shear walls, the normalized axial load values $\left(N/\left(A_g f_{co}\right)\right)$ are generally about 0.1 or less. The presence or absence of axial load does not have a significant effect on the wall behavior [21-22]. Therefore, Axial load was not applied to the specimens and considered as zero in both the experimental and numerical studies. Cold-formed L shaped steel sheets were embedded into the boundary zones with different configurations as seen in Fig. 1. Twelve steel bars with a 10 mm diameter were used to reinforce the body part of the composite shear walls. Stirrups with 8 mm diameter and 150 mm spacing were applied to confine the boundary zone of the wall; while 8 mm horizontal bars were placed into the web with 150 mm intervals. Concrete compressive strength (f_{co}) was tested with an average of 24.6 MPa, while the modulus of elasticity was in a range of 31.35 GPa. Moreover, S420 steel rebars and S275JR cold-formed steel sheets were used to reinforce the composite shear walls. The average yield and ultimate strengths of steel members could be seen in Table 1. The steel elasticity modulus was calculated around 210 GPa for all samples.

Table 1: Steel rebars and sheets properties

Type	Rebar diameter / Steel thickness (mm)	f_y (MPa)	f_u (MPa)
Steel rebars	8	426.0	540.3
	10	463.0	565.3
	12	481.0	588.6
Steel sheets	2 and 3	270.7	351.2

The experimental program used force-controlled and displacement-controlled protocols to apply the quasi-static cyclic lateral load on the composite shear walls. However, considering that the numerical model requires a displacement load history to perform the analysis the loading protocol shown in Fig.2 was extracted from the experiment and used in this study starting from 0.02% drift ratio and increasing about 25% for each step. The details of the experiment setup could be found in references [11-12].

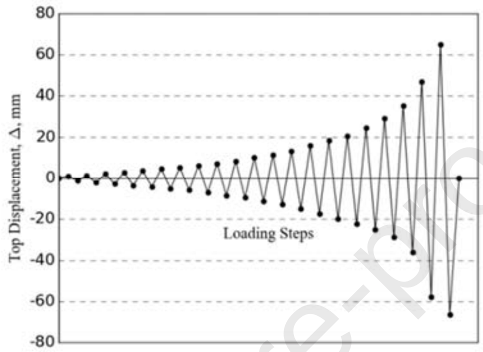

Fig. 2 Applied load protocol for CSW

3. Modeling of nonlinear behavior of CSW

3.1. Review of RC wall modeling

Macroscopic and Microscopic modeling techniques are two groups of modeling approaches used for simulating the behavior of RC structural walls in general. Microscopic models depend mostly on the Finite Element Method (FEM), considered as the most accurate modeling approach for shear walls.

However, the effort required to develop the model (pre-process), the needed analyzing power (computational time) to solve the model, and the post-processing examination of the results is significant, especially for simulating large structures with earthquake loadings. On the other hand, macroscopic models have the simplicity and practicality along with the reasonably required CPU time in comparison with the micro-scale models [23-24]. However, they need special care while selecting materials constitutive models and related parameters to reflect the actual behavior of the materials in use for the required application.

In this study, the Fiber Beam-Column Element Model (FBCEM) was adapted to evaluate the nonlinear behavior of composite shear walls as macroscopic modeling approach, and the implementation of FBCEM in OpenSees [20] was used to examine CSWs under cyclic loads. In this method, the flexural response of the composite shear walls was determined by using a section of the wall divided into macro-fibers representing the concrete and steels in the section based on constitutive stress-strain relationships. Furthermore, the shear response was calculated using a backbone of lateral force-displacement relation applied to a horizontal spring.

3.2. Fiber Beam-Column Element Model

The fiber beam-column element model (FBCEM), introduced by Spacone et al. [25], is one of the widely used and highly reliable methods to simulate concrete columns and shear wall elements under static and dynamic loadings. The model consists of integration points along the element where displacements and forces are calculated using integrals of the cross-sectional parts (Fig. 3.b). Cross-sections at each integration point are divided into multiple fibers representing the stress-strain behavior for each individual material used in the element [25]. For instance, four different materials are utilized (confined concrete, unconfined concrete, reinforcing steel, and steel sheets) to define the response of the fibers in the member’s section as seen in Fig. 3.c.

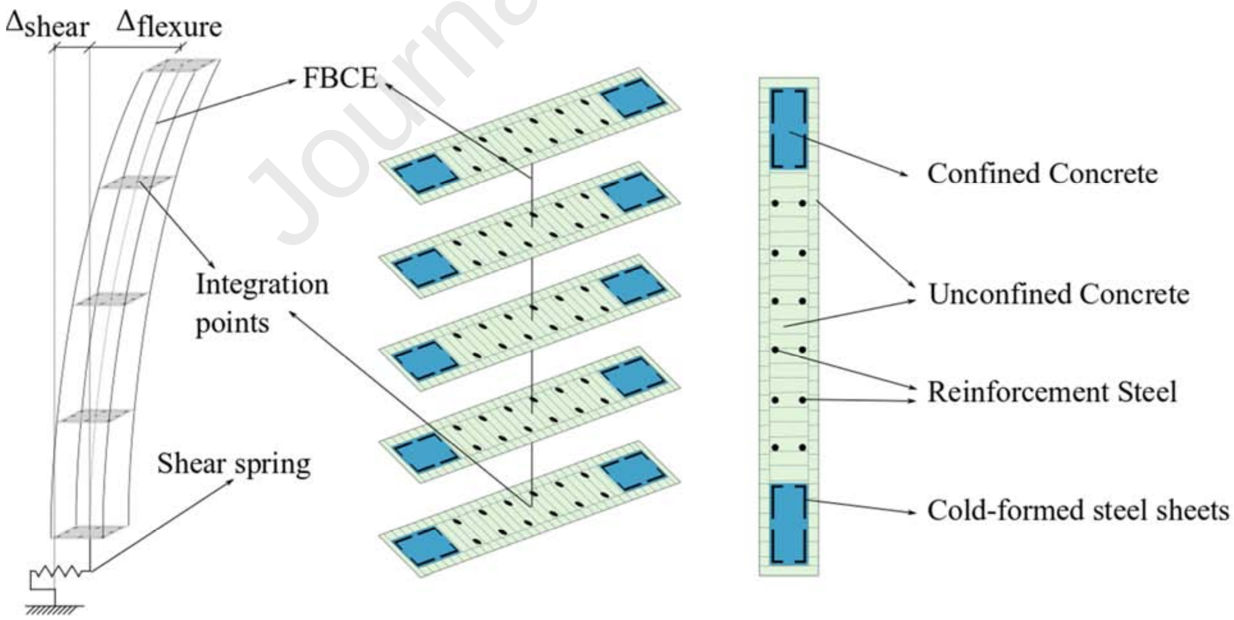

a) b) c)

Fig. 3 Illustration of Fiber Beam-Column Element Model

3.3. Element Formulations

Force-based and displacement-based elements are both distributed-plasticity beam-column formulations commonly used in FBCEM and available in OpenSees [20]. The displacement-based formula assumes a linear distribution of curvature, which requires finer mesh to capture deformations in highly plastic regions [26]. In contrast, the force-based element uses exact solutions for forces, and it allows the use of one element to represent the member for this. However, more CPU time is required with force-based elements and the solution is highly sensitive to the number of integration points. Regularized material constitutive models are also needed to provide accurate simulation [27]. In this study, the displacement-based beam-column element was selected to model the composite shear wall with steel sheets. A total of six elements ("dispBeamColumn" OpenSees element) with 3 integration points for each element were specified to represent CSWs.

3.4. Material Models

Different types of material models are available in the OpenSees library [28]. In this study, Concrete01 and Concrete04 uniaxial materials were selected to define the unconfined and confined concrete material models, respectively. Concrete01 uniaxial material was used to construct Kent and Park [29] unconfined concrete model with peak stress point equals to concrete compressive strength, f_{co}, and the corresponding strain $\varepsilon_{co} = 0.002$. In addition, unconfined concrete ultimate strain at the end of the descending line was set to 0.007 (Fig. 4.a) at which the analysis process was considered to be finished.

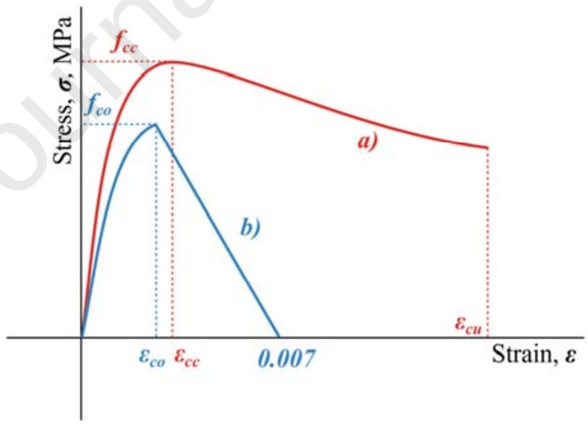

Fig. 4 a) Confined and b) Unconfined concrete model envelops

The stress-strain concrete model developed by Mander et al. [30] was adapted for the confined concrete at boundary zones of the composite shear walls. Considering that mathematical confinement models for concrete surrounded with steel sheets or sections could not be found in the literature, the concrete in boundary zones were accepted to be confided only with the transverse reinforcement. Concrete04 uniaxial material was selected from the OpenSees library to construct a confined concrete model (Fig. 4.b) where peak stress (f_{cc}) and strain (ε_{cc}) were calculated according to Mander et al. [30]. Tension strength was neglected for both confined and unconfined concrete.

Whereas composite shear wall cyclic behavior was meanly dominated by steel response to lateral loads, three different uniaxial steel models were selected and tested against the experimental results of CSW2 and presented in Fig. 5. Steel01 produced a bilinear steel material with elastic branch and had initial elastic tangent equaled to the modules of elasticity (E_s) and plastic branch with tangent equaled to bE_s, where b was the strain hardening ratio (Fig. 5.a). Steel02 constructed Menegotto and Pinto's [31] steel material with several parameters that described and controlled elastic to plastic transition and stiffness degradation (Fig 5.b). The hysteretic material model found in Opensees, based on Takeda et al. [32] and Filippou et al. [33], was a three-axis uniaxial material in which strain hardening, hardness degradation, pinching, and damage could be defined according to ductility levels. In this model, the unloading stiffness was determined using $\mu_i^{-\beta} * E_s$, where μ_i was ductility level and β was the modification parameter (Fig. 5.c). Furthermore, $Pinch_x$ and $Pinch_y$ were pinching factors for strain and stress, respectively, during reloading stages. These factors could be used to include stiffness reduction during reloading occurred because of crack opening and buckling of steel reinforcing bars and composite sheets. Also, they take into account the effect of stiffness restoration after cracks were closed and steel elements were recovered. As seen from Fig. 5, the first two models (Steel01 and Steel02) overestimated the energy dissipation of the members as they could not take the effects that caused pinching into account. On the other hand, the Hysteretic model, with the default parameters settings from OpenSees (Fig. 5.c), was able to fairly capture the cyclic behavior of CSW. Moreover, as seen in Fig. 6, the simulation ability of the model was regulated by modifying β, $Pinch_x$ and $Pinch_y$ to re-estimate the unloading stiffness and pinching based on ductility levels. For this study, the hysteretic steel model was adopted and regulated to analyze the response of composite shear walls under cycling loadings, and β, $Pinch_x$ and $Pinch_y$ were determined as 0.20, 0.25 and 0.15 respectively.

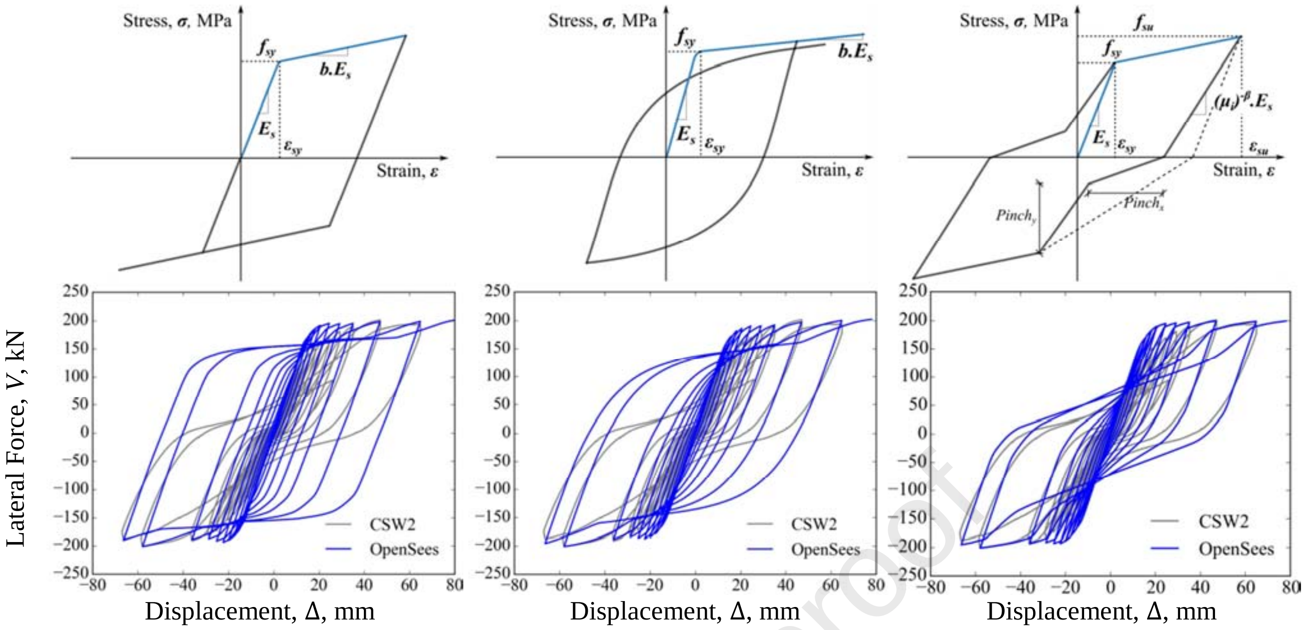

a) elasto-plasto (Steel01) b) Menegotto and Pinto (Steel02) c) Hysteretic model

Fig. 5 Comparison of the experimental results and OpenSees analyses with the selected three steel models

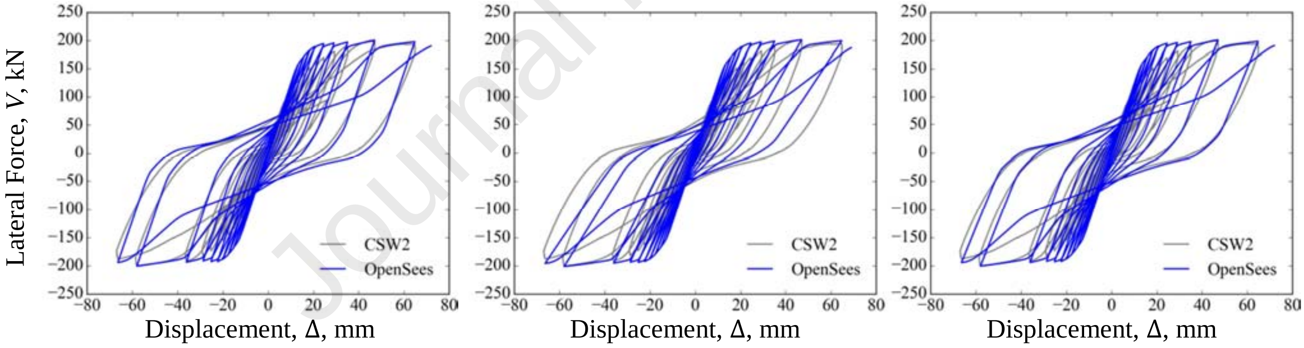

$\beta = 0.00$ $\beta = 0.60$ $\beta = 0.20$

Fig. 6 Hysteretic model parameters regulation

3.5. Constitutive Shear Model

Although fiber beam-column elements models could simulate the axial-flexure coupled interaction based on sectional analysis [34], the shear response cannot be calculated from FBCEM. For that reason, shear spring is inserted within the model connecting the two nodes at the base of the member (Fig. 3). Shear force-displacement relationship is applied to that spring to simulate shear deformations. However, linear, bilinear, trilinear, or more sophisticated models are used in the literature to define the constitutive shear model [35]. For simplicity purposes, the linear relation was adopted in this work with uncracked shear stiffness calculated as per Eq. 1.

$$Shear\ Stiffness = G_c A = \frac{E_c}{2(1+\nu)} A_{cv} \quad (1)$$

where; ν is Poisson's ratio and taken as 0.2, and A_{cv} is the area of the section. While the effective shear stiffness (GA_{eff}) could be taken as 0.1 or 0.05 form $G_c A$ according to PEER and ACT [36]. As seen in Fig. 7, considering $GA_{eff} = 0.1 G_c A$ is the closest approach in term of stiffness to determine the shear response of CSW2, this value was selected for the simulation in this work.

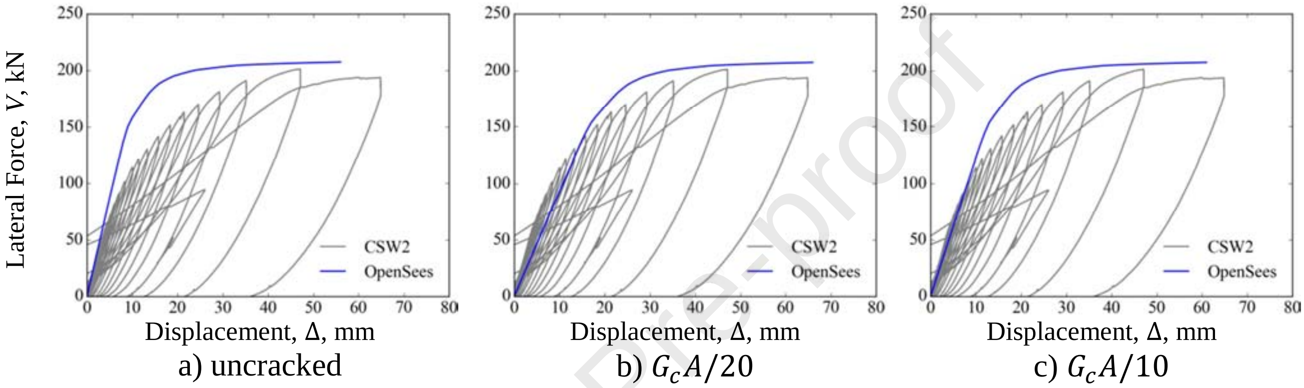

Fig. 7 The influence of effective shear stiffness on the total response of RC shear walls

3.6. Model validation

In this work, a numerical model was formed by using displacement-based force beam-column elements with a shear spring model to simulate the total response of composite shear walls. The outcomes of the numerical analysis using the selected parameters were compared with experimental results for three different composite shear walls. As can be seen from Fig. 8, the numerical model was very successful to simulate the total response of CSW2 and CSW3 specimens, while CSW1 simulation had slight differences in terms of capacity and cyclic behavior.

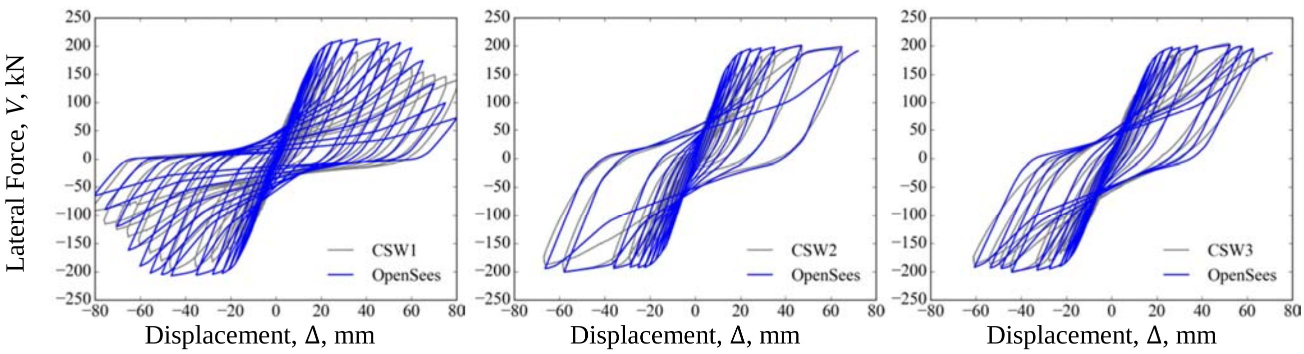

Fig. 8 Performance of the numerical model

According to the definitions from Fig. 9a, tabulated data in Table 2 summarizes the main backbone figures from the OpenSees model compared to test results. In table 2, V_{max} is the maximum lateral load capacity, Δ_y, Δ_{max}, and Δ_u are displacements at yield, maximum load, and ultimate load (85% of V_{max}), respectively. By taking the ratios of the model results to experimental results, it became clear that the numerical model could simulate the total response of composite shear walls to a great extent.

Moreover, the cumulative dissipated energy by elements was calculated by adding areas defined by the curve of the lateral load-displacement loops as seen from Fig. 9b. The dissipated energies for the numerical and experimental hysteric curves were plotted to compare in Fig. 10. As seen from the figure, the numerical model captured the energy dissipation behavior extremely well with variances in the total energy about 7.8%, 2.9%, and 6.8% for CSW1, CSW2, and CSW3, respectively. According to the validation study, it was concluded that the constructed OpenSees based numerical model could be used efficiently to determine the behavior of composite shear walls with cold-formed steel sheets.

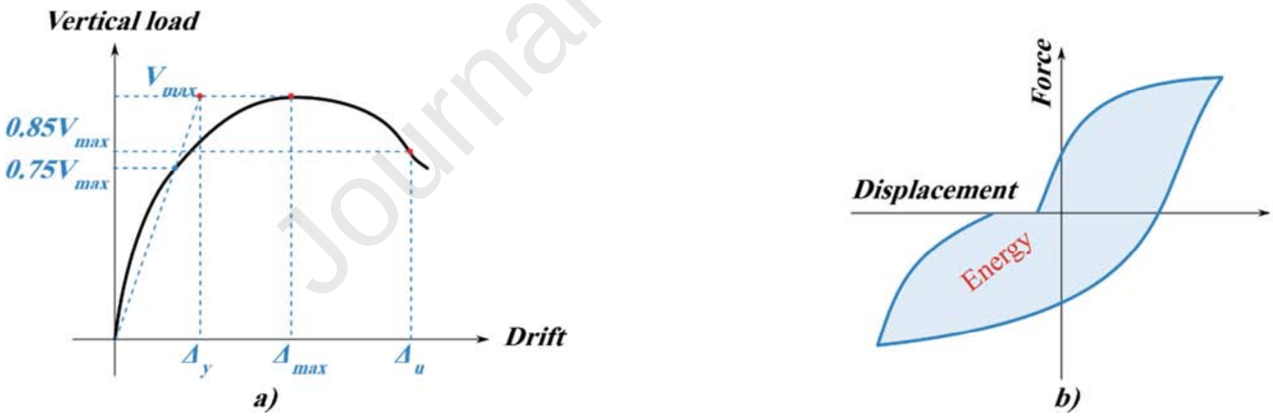

Fig. 9 ***a)*** Definition of main drifts points on the lateral load-displacement envelope, ***b)*** Energy dissipation calculation for one loop

Table 2: Comparison between the numerical model and experimental results

Wall		Δ_y	$\frac{\Delta_y}{\Delta_y^{Exp.}}$	Δ_{max}	$\frac{\Delta_{max}}{\Delta_{max}^{Exp.}}$	V_{max}	$\frac{V_{max}}{V_{max}^{Exp.}}$	Δ_u	$\frac{\Delta_u}{\Delta_u^{Exp.}}$
CSW1	Num.	-17.9	0.77	-46.2	1.00	-206.1	1.04	-59.1	1.07
	Exp.	-23.2		-46.2		-198.0		-55.3	
CSW2	Num.	-16.2	0.64	-57.9	1.00	-199.2	0.99	-66.4	0.99
	Exp.	-25.3		-57.9		-200.7		-66.9	
CSW3	Num.	19.0	0.80	52.3	1.00	199.0	0.98	74.0	1.08
	Exp.	23.8		52.3		203.4		68.5	

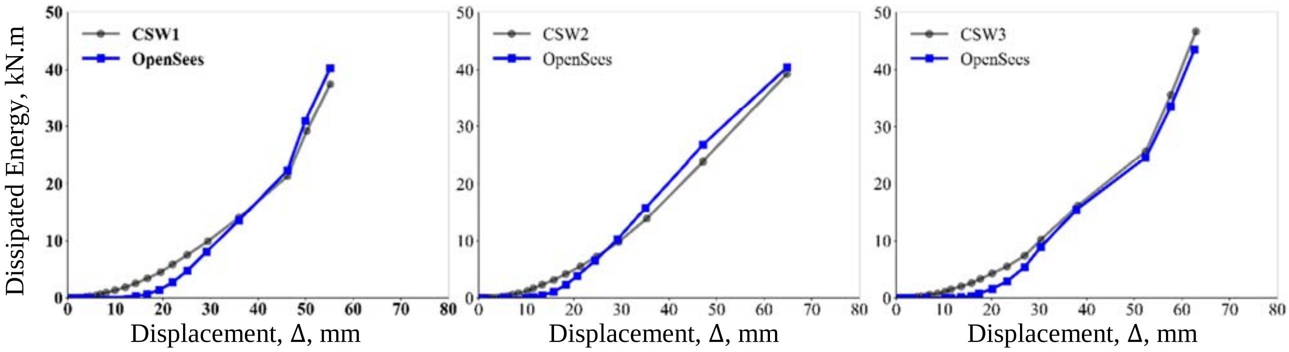

Fig. 10 Cumulative energy dissipation of experimental and the numerical model

4. Parametric study

A parametric study was performed to investigate L-shaped steel sheets properties on the lateral behavior of composite shear walls, where steel reinforcement bars were replaced with cold-formed steel sheets (CFSS) at the boundary zone of RC shear walls. For that purpose, CFSS thickness and yield strengths were selected as the main parameters in this study. As seen in Table 3, a total of 18 different models were created with different combinations of the selected parameters.

Table 3: Models properties of the parametric study

Section Type	t_{CFSS} ***(mm)***	f_{yCFSS} ***(MPa)***
S1 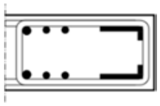	5.0	270.0
		360.0
		480.0
	7.0	270.0
		360.0
		480.0
S2 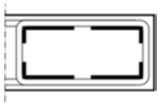	5.0	270.0
		360.0
		480.0
	7.0	270.0
		360.0
		480.0
S3 	5.0	270.0
		360.0
		480.0
	7.0	270.0
		360.0
		480.0

On the other hand, mechanical properties of concrete, longitudinal, and transverse bars were kept constant to agree with the experimental study. Although three different sections were chosen and named as S1, S2, and S3 according to specimens CSW1, CSW2, and CSW3, respectively (Table 3), cold-formed steel sheets dimensions were kept fixed for comparison reasons, and L19.0x57.0 was used for all the sections. Cyclic loading was applied to determine the lateral load-displacement relationships for the eighteen models, and the analyses were terminated upon reaching unconfined concrete ultimate strain. Envelope curves were used for easier comparisons with different parameters.

5. Results and Discussion

The results of the eighteen composite shear wall models in terms of the lateral load-displacement relationships are illustrated in Fig. 11. The effects of thicknesses and yield strength of cold-formed steel sheets (CFSS) on the response of the walls under lateral loading are discussed.

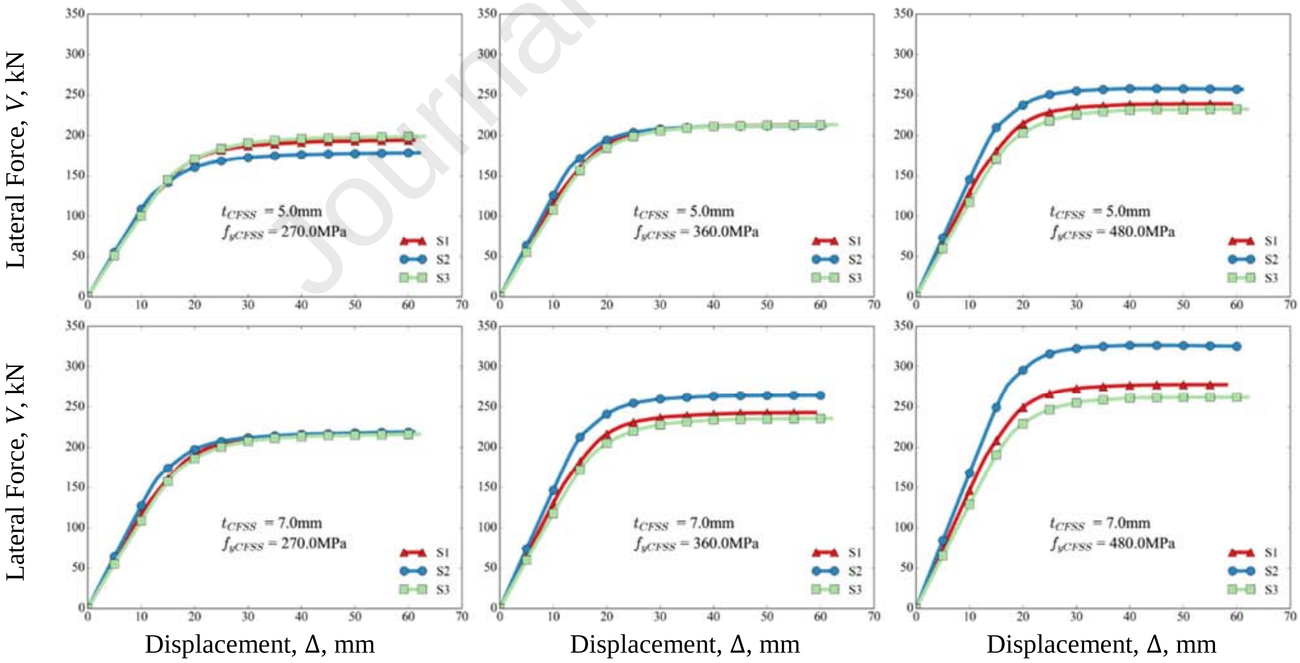

Fig. 11 The lateral force and displacement relationship of composite RC shear wall

Generally, the lateral load capacity of composite shear walls can be adjusted by increasing the cold-form steel sheets thicknesses and yield strength at the tension boundary regions of the CSWs. For instance, S2 with configuration based on CSW2 has a lateral load capacity of 219.0 kN for CFSS thickness of 7 mm and f_y=270.0 MPa, while the capacity increased 49% for f_y=480.0 MPa and reached 327 kN. Contrariwise, for the CFSS thickness of 5 mm, the lateral load capacity is 178 kN and increased 45% to reach 258.0 kN for the same increment of CFSS yield strength from 270.0 to 480.0 MPa, respectively. Likewise, lateral capacity for section S3 when CFSS thickness is 7 mm and f_y=270.0 MPa is 198.0 kN and increased 19% to reach 236.0 kN while f_y increased to 480.0 MPa. On the other hand, the lateral load capacity for the same section configurations is 216.0 kN for CFSS thickness of 5 mm and f_y=270.0 MPa, while the capacity increased 21% for f_y=480.0 MPa and reached 262.0 kN. In addition, for constant CFSS yield strength of 480.0 MPa and while the CFSS thicknesses increased from 5 mm to 7 mm; lateral load capacity for section S1 is increased 16% and reached 278.0 kN, S2 capacity increased 27% and reached 327.0 kN, and for S3 the increment is 11% to reach 262.0 kN.

As seen in Fig. 11, the lateral load capacity varied considerably with the change in CFSS yield strength and thickness for the specimen with the S2 section but slightly for S1 and S3. On the other hand, the investigated parameters of the cold-formed steel sheets influenced the lateral load capacity of CSW1 based section S1 more than the lateral load capacity of section S3. Since the cold-formed steel sheets (CFSS) were located at the outermost side of the boundary regions of the composite shear wall cross-section in S1 (CSW1), CFSS elements resisted the bending moments about the strong axis by using all their section capacities. However, since the CFSS elements were not located at that outermost side of the composite shear wall's cross-section, they could not use their sections full plastic moment capacities to resist bending moments for the section S3 (CSW3).

Additionally, the cover concrete was spalled when all the samples reached about 60 mm. Therefore, it is determined that the variation of CFSS thicknesses and yield strength at the tension boundary regions has no significant effect on the displacement capacity of composite shear walls. On the other hand, the ductility of the wall increases positively because of the positive effect of the increase in thickness and yield strength of CFSS on both horizontal load capacity and stiffness. Furthermore, when comparing the use of longitudinal reinforcement and cold-formed steel sheet (CFSS) in the outer side of the tension boundary zone, it is clearly seen from the numerical analysis results that CFSS elements have a positive effect on the composite wall behavior in terms of strength capacity, stiffness, and ductility.

6. Conclusion

This paper focused on the behavior of composite shear walls with L-shaped cold-formed steel sheets. In order to investigate the behavior of the composite shear walls, a numerical model based on the OpenSees platform was developed and validated in comparison to experimental results. L-shaped cold-formed steel sheets thickness and yield strength were parametrically studied by using the developed numerical model to better understand their effect on the total response of CSW. The following conclusions could be derived from this work as follows:

1. The macroscopic modeling technique showed a reliable performance in simulating the nonlinear behavior of composite shear walls. The developed OpenSees based numerical model was simple to build and very practical in conducting the parametric study with very short analysis time and minimum convergence errors. Additionally, the numerical model's ability to simulate the real response of CSW could be increased by using a more sophisticated shear model and by taking the slip of steel elements into account.
2. Furthermore, the pinching effect captured by the developed model in load-displacement hysteresis curves appears explicitly unlike previous numerical studies that used microscopic methods without considering this behavior. For that reason, the overall agreement between the experimental and numerical results is excellent in terms of dissipated energy prediction and calculations which were obtained by taking the hysteric loops shape into account and as a summation of the enclosed area for each cycle.
3. The parametric investigation showed that increasing the yield strength of CFSS without changing the thickness positively affected the lateral load capacity for all composite shear wall samples as expected. However, these changes varied with steel configurations in the border regions and were noticed in sections with higher L-shaped CFSS ratios.

4. The influence of the cold-formed steel sheets thickness was also obvious on the behavior of CSWs since the capacity of the walls becomes larger with the increasing of the CFSS thicknesses value. Nevertheless, this effect was correlated with the yield strength of the sheets since it was more apparent with higher values of f_{yCFSS}.

5. As a result, increasing the thicknesses and yield strengths of CFSS elements at the boundary regions of the composite shear walls will improve the total response of the CSWs under lateral loads, and in turn, will affect the load capacity of the entire structure. Moreover, placing cold-formed steel sheets on the outer side of boundary regions could effectively improve the flexural capacity of the composite shear wall according to the results of the experimental and parametric studies. Thus, using the S2 configuration type of CSW has more advantages than the other two

types in case of using higher thicknesses of CFSS to prevent buckling of the outer elements.

References

[1] Qian, J., Jiang, Z., & Ji, X. (2012). Behavior of steel tube-reinforced concrete composite walls subjected to high axial force and cyclic loading. Engineering Structures, 36, 173–184.

[2] Cho, S. H., Tupper, B., Cook, W. D., & Mitchell, D. (2004). Structural steel boundary elements for ductile concrete walls. Journal of Structural Engineering, 130(5), 762–768.

[3] Zhao, Q., & Astaneh-Asl, A. (2007). Seismic behavior of composite shear wall systems and application of smart structures technology. Steel Structures, 7, 69–75.

[4] Hu, H.-S., Nie, J.-G., Fan, J.-S., Tao, M.-X., Wang, Y.-H., & Li, S.-Y. (2016). Seismic behavior of CFST-enhanced steel plate-reinforced concrete shear walls. Journal of Constructional Steel Research, 119, 176–189.

[5] Zhang, X., Qin, Y., & Chen, Z. (2016). Experimental seismic behavior of innovative composite shear walls. Journal of Constructional Steel Research, 116, 218–232.

[6] Cheng, C., & Zhou, D. (2015). Experimental study on seismic behavior of composite concrete and double-steel-plate shear walls with binding bars. 6th International Conference on Advances in Experimental Structural Engineering & 11th International Workshop on Advanced Smart Materials and Smart Structures Technology. August 1-2.

[7] Liao, F.-Y., Han, L.-H., & Tao, Z. (2012). Performance of reinforced concrete shear walls with steel reinforced concrete boundary columns. Engineering Structures, 44, 186–209.

[8] Dan, D., Fabian, A., & Stoian, V. (2011). Theoretical and experimental study on composite steel-concrete shear walls with vertical steel encased profiles. Journal of Constructional Steel Research, 67(5), 800–813.

[9] Arabzadeh, A., Soltani, M., & Ayazi, A. (2011). Experimental investigation of composite shear walls under shear loadings. Thin-Walled Structures, 49(7), 842–854.

[10] Yuksel, S. B., & Unal, A. (2015). Experimental Behavior of Composite Shear Walls Having L Shape Steel Sections in Boundary Regions. World Academy of Science, Engineering, and Technology, International Journal of Civil, Environmental, Structural, Construction, and Architectural Engineering, 9(6), 747-752.

[11] Kisa, M. H. (2020). An experimental study on hysteric behavior of composite shear walls with vertical cold-formed steel sheets. PhD thesis, Sakarya University, Turkey (In Turkish).

[12] Kisa, M. H., Yuksel, S. B., & Caglar, N. (2021). Experimental study on hysteric behavior of composite shear walls with steel sheets. Journal of Building Engineering, 33, 101570.

[13] Wang, B., Jiang, H., & Lu, X. (2017). Seismic Performance of steel plate Reinforced Concrete shear wall and its application in China Mainland. Journal of Constructional Steel Research, 131, 132-143.

[14] Elmatzoglou, M., & Avdelas, A. (2017). Numerical modelling of double-steel plate composite shear walls. Computation, 5(1), 12.

[15] Nguyen, N. H., & Whittaker, A. S. (2017). Numerical modelling of steel-plate concrete composite shear walls. Engineering Structures, 150, 1–11.

[16] Zhou, D., Liu, L., & Zhu, L. (2016). Lateral load-carrying capacity analyses of composite shear walls with double steel plates and filled concrete with binding bars. Journal of Central South University, 23(8), 2083–2091.

[17] Cho, S. G., Park, W.-K., So, G.-H., Yi, S.-T., & Kim, D. (2015). Seismic capacity estimation of Steel Plate Concrete (SC) shear wall specimens by nonlinear static analyses. KSCE Journal of Civil Engineering, 19(3), 698–709.

[18] Ali, A., Kim, D., & Cho, S. G. (2013). Modeling of nonlinear cyclic load behavior of I-shaped composite steel-concrete shear walls of nuclear power plants. Nuclear Engineering and Technology, 45(1), 89–98.

[19] Zhou, Y., Lu, X., Huang, Z., & Bo, Y. (2010). Seismic behavior of composite shear walls with multi-embedded steel sections. Part II: analysis. The Structural Design of Tall and Special Buildings, 19(6), 637–655.

[20] McKenna, F., Fenves, G. L., & Scott, M. H. (2000). Open system for earthquake engineering simulation (OpenSees). Pacific Earthquake Engineering Research Center, University of California, Berkeley, CA.

[21] Christidis, K. I., & Trezos, K. G. (2017). Experimental investigation of existing non-conforming RC shear walls. Engineering Structures, 140, 26–38.

[22] Shegay, A. V., Motter, C. J., Elwood, K. J., Henry, R. S., Lehman, D. E., & Lowes, L. N. (2018). Impact of axial load on the seismic response of rectangular walls. Journal of Structural Engineering, 144(8), 04018124.

[23] Martinelli, L. (2008). Modeling shear-flexure interaction in reinforced concrete elements subjected to cyclic lateral loading. Structural Journal, 105(6), 675–684.

[24] Jalali, A., & Dashti, F. (2010). Nonlinear behavior of reinforced concrete shear walls using macroscopic and microscopic models. Engineering Structures, 32, 2959–2968.

[25] Spacone, E., Filippou, F. C., & Taucer, F. F. (1996). Fibre beam-column model for non-linear analysis of R/C frames: Part I. Formulation. Earthquake Engineering & Structural Dynamics, 25(7), 711–725.

[26] Wu, Y.-T., Lan, T.-Q., Xiao, Y., & Yang, Y.-B. (2017). Macro-Modeling of Reinforced Concrete Structural Walls: State-of-the-Art. Journal of Earthquake Engineering, 21(4), 652–678.

[27] Pugh, J. S., Lowes, L. N., & Lehman, D. E. (2015). Nonlinear line-element modeling of flexural reinforced concrete walls. Engineering Structures, 104, 174–192.

[28] Mazzoni, S., McKenna, F., Scott, M. H., & Fenves, G. L. (2007). OpenSees command language manual. Pacific Earthquake Engineering Research (PEER) Center, 264.

[29] Kent, D. C., & Park, R. (1971). Flexural members with confined concrete. Journal of the Structural Division.

[30] Mander, J. B., Priestley, M. J. N., & Park, R. (1988). Theoretical Stress-Strain Model for Confined Concrete. Journal of Structural Engineering, 114(8), 1804–1826.

[31] Menegotto, M., & Pinto, P. (1973). Method of Analysis for Cyclically Loaded Reinforced Concrete Plane Frames Including Changes in Geometry and Non-elastic Behavior of Elements Under Combined Normal Force and Bending. Proceedings. IABSE Symposium on Resistance and Ultimate Deformability of Structures Acted on by Well-Defined Repeated Loads. Presented at the Lisbon, Portugal. Lisbon, Portugal.

[32] Takeda, T., Sozen, M. A., & Nielsen, N. N. (1970). Reinforced concrete response to simulated earthquakes. Journal of the Structural Division, 96(12), 2557–2573.

[33] Filippou, F. C., d'Ambrisi, A., & Issa, A. (1992). Nonlinear static and dynamic analysis of RC subassemblages. Rep. No. UCB/EERC-92, 8.

[34] Galal, K., & El-Sokkary, H. (2008). Advancement in Modeling of RC Shear Walls. 14th World Conference on Earthquake Engineering, (October).

[35] Kolozvari, K., & Wallace, J. W. (2016). Practical Nonlinear Modeling of Reinforced Concrete Structural Walls. Journal of Structural Engineering, 142(12), G4016001.

[36] PEER, & ACT. (2010). Modeling and acceptance criteria for seismic design and analysis of tall buildings, Task 7 Report for the Tall Buildings Initiative (PEER Report No. 2010/111). Richmond, California: Pacific Earthquake Engineering Research Center.

Highlights

- Composite shear walls with L- shaped cold-formed steel sheets are numerically investigated.
- OpenSees based numerical model is developed and verified with experimental results.
- Parametric study is conducted to investigate the effect of CFSS properties on the response of CSW.

Journal Pre-proof

Declaration of interests

☒ The authors declare that they have no known competing financial interests or personal relationships that could have appeared to influence the work reported in this paper.

☐The authors declare the following financial interests/personal relationships which may be considered as potential competing interests: